Air and gas pockets in sewerage pressure mains

C.L. Lubbers* and F. Clemens**

*WL | Delft Hydraulics, P.O. Box 177, 2600 MH Delft, The Netherlands (E-mail: *christof.lubbers@wldelft.nl*)

**Delft University of Technology, Faculty of Civil Engineering and Geosciences, Section of Sanitary Engineering, P.O. Box 5048, 2600 GA Delft, The Netherlands (E-mail: *f.h.l.r.clemens@citg.tudelft.nl*)

Abstract In The Netherlands, wastewater is collected in municipal areas and transported to large centralised WWTPs by means of an extensive system of pressure mains. Over the past decades these pressure mains did not receive much attention in terms of monitoring of performance or maintenance.
For that reason, in practice their state of functioning is often not known. Failure of operation is only noticed when the capacity of the system proves to be insufficient to fulfil the minimum design capacity demand.
A recent inventory showed that half of the pressure mains show an increased pressure loss for no directly obvious reason. Many causes may account for the reduction of the system's nominal capacity like an increased wall roughness, scaling or occurrence of free gas in the pipeline. The occurrence of free gas may be caused by degassing of dissolved (bio) gas or by air entrained at the pumps' inlet or at air valves.
A research study is started that will focus on three main issues:

- The description of the gas-water phenomena in wastewater pressure mains with respect to transportation and dynamic hydraulic behaviour,
- A method to diagnose gas problems, and
- To overcome future problems by either applying remedial measures or improving the design of wastewater pressure systems.

For this study, two experimental facilities are constructed, a small circuit for the study of multi-phase flow and a second, larger one for the research into diagnostic methods. This paper describes the preliminary results of the experiments in the multi-phase circuit.

Keywords Air pockets; experimental research; pressure mains

Introduction

The hydraulic capacity of pressure mains does change during their operational life because of scaling, the occurrence of air/gas pockets, wear of pumps, etc. In practical cases it is no trivial task to identify the cause of capacity loss in the first place. To find a sound solution for a 'problematic' pressure main is in many cases even more difficult since in a significant number of cases a basic design problem seems to be the cause. Free gas in pressurised pipelines/mains can significantly reduce the flow capacity. When the capacity of wastewater pressure mains fails to be in line with the design value, undesirable spills or efficiency loss may be the result.

Delft Hydraulics and Delft University started an extensive research programme in 2003 in the processes. The objectives of this programme are:

- Developing a method to quickly diagnose the cause of capacity loss of a pressure main.
- Get insight into the processes and main parameters influencing scaling.
- A quantitative understanding of the processes involved in the dynamics of air/gas pockets in pressure mains.
- Obtain a better code of design practice in terms of avoiding scaling and the occurrence of persistent air/gas pockets in pressure mains.

In this paper only the third objective mentioned is addressed, discussing preliminary results only.

Water Science & Technology **Vol 52 No 3 pp 37–44**

At present, only little is known about the influence of the wastewater properties on the transport of air/gas pockets in pressure mains when compared to clean water. The generally used equations for critical velocity of gas transport (e.g. Kent, 1952; Wisner, 1975; Walski, 1994) are based on experiments carried out with clean water and small pipe diameters. It is likely that for wastewater with its divergent properties compared to clean water these equations are not valid. Figure 1 shows the differences in critical velocity given in the literature. Some preliminary results of the Delft experiments are indicated also.

Experimental set-up

The experiments are conducted in a dedicated facility for research on air/gas pockets that are located at the transition from horizontal to inclined pipes. The facility (Figure 2) is specially designed to inject a controlled and monitored airflow into the liquid phase. From a constant head reservoir a pump circulates water through the experimental facility. A flow control valve (FCV) in combination with an electromagnetic flowmeter (EMF) and PC adjust the flow rate to its set value. Air is supplied by the standard 6 bar pressurised air-infrastructure in the building. A combined mass flowmeter and FCV adjusts the airflow to its set value. Since the air flowmeter measures mass, the output gives 'nl/min', i.e. a volumetric flow rate at normal conditions (101,325 Pa and 0 °C). The test section consists of a horizontal section, at the air injection point a downward sloping section is followed by a horizontal section. The test section is made of transparent material (Perspex) with an inner diameter of 220 mm. Flexible hoses connect the test section to the reservoir and pump. The water/air mixture returns to the reservoir over a weir in order to strip as much air as possible from the water. The injection of air into the system results in a head increase of the pump, causing the flow rate to drop. The flow control allows a constant flow rate during head changes.

The facility incorporates the following instrumentation: EMF DN215 (range 0–100 l/s, uncertainty $< 0.25\%$), gas flowmeter (1–50 nl/min, $< 0.5\%$), two absolute pressure transmitters (0–3 bar, $< 0.1\%$), and temperature transmitter (3–100 °C, < 0.1 °C).

The absolute pressure transmitters are located in the horizontal parts of the test sections. In order to prevent air from disturbing the pressure measurements, the tapping is located at the bottom of the pipe. The temperature transmitter is located at the reservoir in order to monitor possible temperature increase caused by the pump.

All signals are recorded using an automated data-acquisition system in which the sampling frequency can be adjusted manually ranging between 0 and 10 kHz; the acquired data are stored on a hard disk.

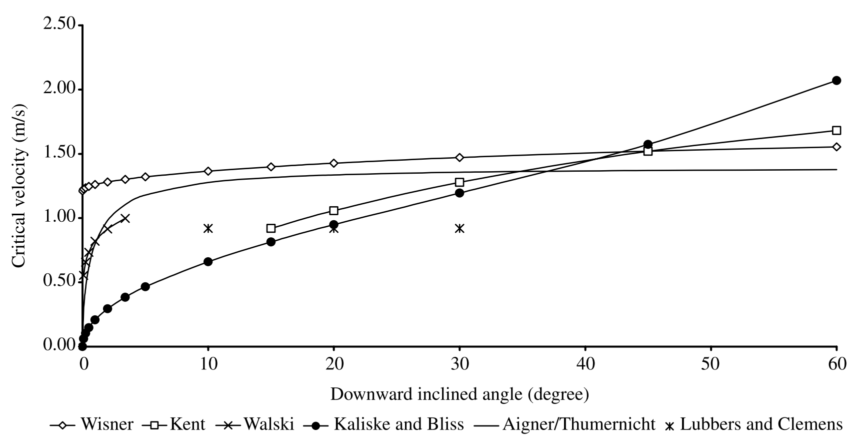

Figure 1 Critical velocity as a function of pipe angle

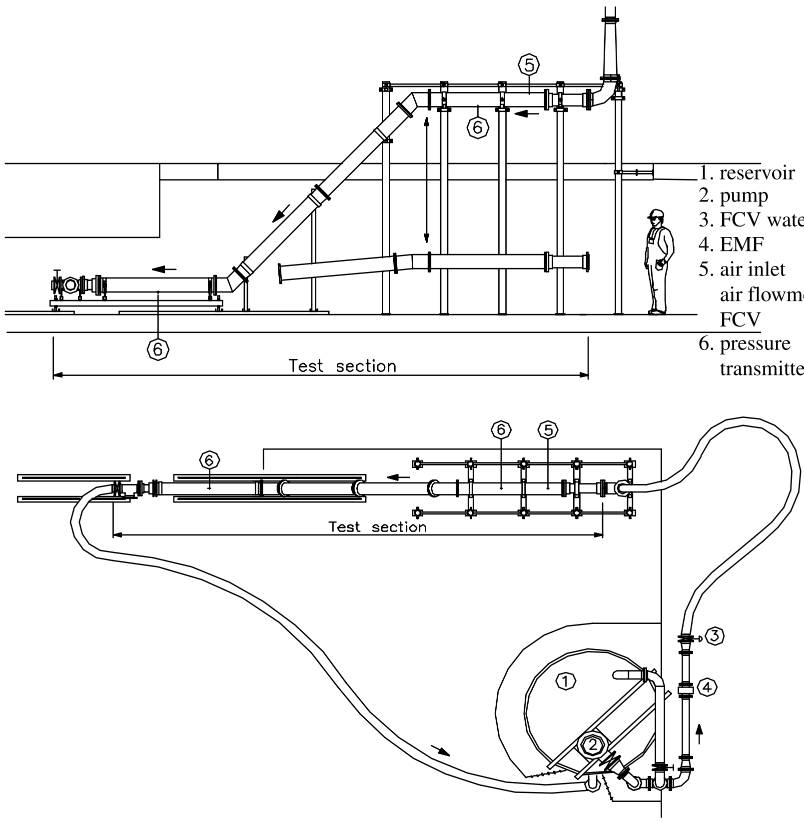

Figure 2 Top and side view of the experimental set-up

Transport modes of air/gas pockets

The processes involved in air/gas transport in water are well known and not very complex in themselves:

- Buoyancy
- Drag
- Equilibrium in surface tensions (water/air/wall)

Yet studying the transport under stationary conditions (constant water and air/gas discharge) reveals that chaotic behaviour occurs. In a downward inclined pipe it is seen that at low concentrations of air/gas the air bubbles stay small (order of magnitude 10 mm), these bubbles have a high drag/buoyancy ratio (Figure 3, left). When either the water discharge decreases or the air discharge increases, bubbles show a tendency to aggregate forming larger bubbles having a small drag/buoyancy ratio (Figure 3, right). This leads for larger airflow rates to a chaotic process in which a stream of large air pockets/plugs flows upward (in the opposite direction to the water flow) while a second stream of smaller bubbles is being transported downward (Figure 4).

Aggregation of air bubbles is a process controlled in part by surface tension and by turbulence; the quantification of this, however, will be investigated in more depth in the rest of the research period. In this ‘dual flow mode’ much energy is lost since in a given cross section a large percentage of this cross section is air.

Another interesting process is the manner in which air/gas pockets are transported in a downward-facing bend.

Small air bubbles are released from the air inlet point. These air bubbles are transported by the water towards the bend. At sufficiently high water velocities, the air

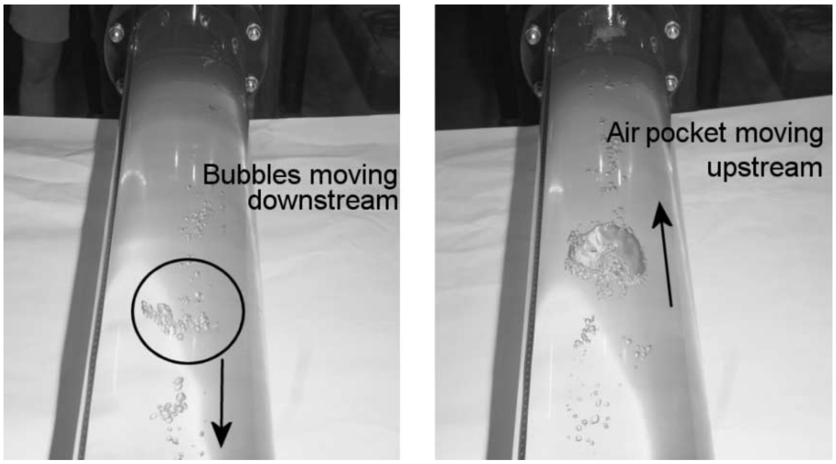

Figure 3 Left: Small bubbles moving downstream, Right: Air pocket moving upstream

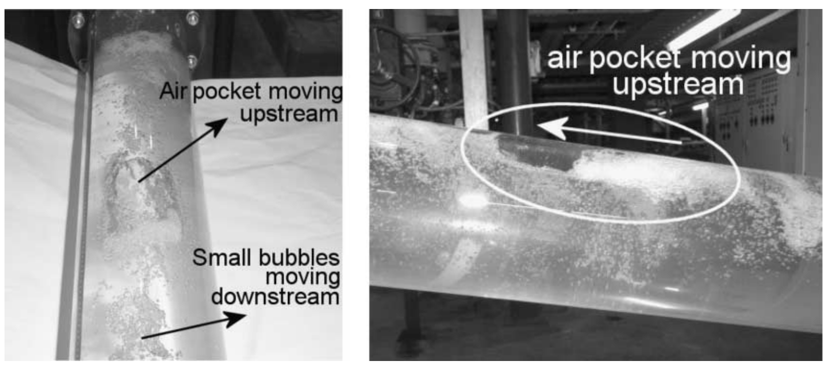

Figure 4 Dual mode flow, large plug moving upstream, small bubbles moving downstream

bubbles pass the bend unhindered and run down the inclined part (Figure 5 left). In this transport mode air transport is controlled by the drag of the water flow on the small air bubbles. At the inclined slope the air bubbles may accumulate into larger air pockets that run upstream if their size is large enough, because of their increased buoyancy/drag ratio. This air pocket stretches from upstream of the bend and forms a 'buffer' (Figure 5 right). Now, the small air bubbles introduced at the inlet first merge with the air pocket in the bend. Small air bubbles that are ripped from the tail of the air pocket by turbulence cause air transport from the 'buffer'; the mechanism for air transport is now different. The presence of an air pocket plays a significant role in the transport of air.

Preliminary results

For three different slopes (30°, 20° and 10°) the head loss between the two pressure transmitters was monitored for a large range of water and air discharges. The time scale at which the phenomena take place ranges from tenths of seconds to hours. Especially the situations close to the critical velocity and small air discharges show a slow adaptation to changed conditions (e.g. larger flow).

Initially, the air discharged from the tail of the 'buffer' may be very close but not equal to the air supply. The air pocket is growing but the growth rate is not visible by eye and can erroneously be taken as stationary. The upstream and downstream pressures are sampled and the pressure difference is plotted during testing on a large time scale.

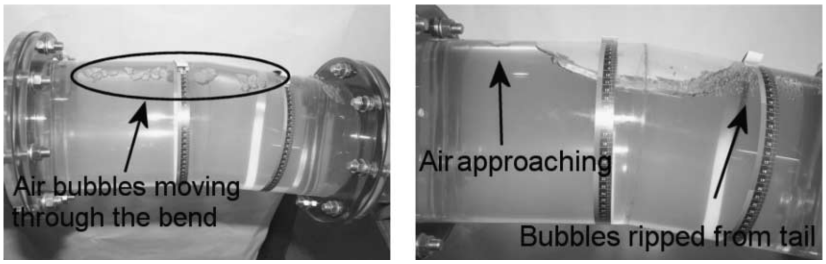

Figure 5 Left shows small air bubbles moving through the bend, Right shows an air pocket acting as buffer

Figure 6 shows an example of a record of an air pocket growing. Only if the pressure differential line is at a constant level, a measurement is taken. As soon as a stationary situation was achieved, the water and air flow rate, the upstream and downstream pressure and the water temperature signals were recorded. All signals have been recorded for 30 seconds with a sample rate of 100 Hz. The sample rate is sufficiently high to follow the 'spikes' in the pressure difference signal (Figure 6). The mean value and standard deviation of the signals are taken per measurement. Further calculations are carried out with the mean values. The energy loss shown in following figures is calculated by subtracting the static head h of the pressure signal p. The total energy loss is defined as:

$$\Delta H_{total} = \frac{(p_1 - p_2)}{\rho g} - (h_1 - h_2),$$

assuming that the velocity head difference between locations 1 and 2 is neglected. After measuring the head loss for only water over the flow range (5 to 65 l/s or 0.15 to 1.70 m/s), the lowest flow rate that could discharge the minimum airflow rate (1 nl/min) was determined. If that resulted in a stationary condition, the airflow rate was increased in steps to the maximum flow rate (49 nl/min). Figure 7 shows the measured total head loss for different water flow rates for the 10° bend.

For all airflow rates, the head loss line seems to decrease linearly with water flow increase to the head loss values corresponding to the pure water values. For the larger airflow rates Figure 7 shows a more gradual transition to the pure water line, especially between 55 and 65 l/s (1.45 – 1.70 m/s). Possibly, this is caused by the air bubble flow which creates a significant head loss (the air pocket at the bend is very small), as opposed to two-phase flow with small airflow rate. For the three tested slopes, the minimum water flow rate that discharges air was around 35 l/s (0.95 m/s) apparently implying no influence of the slope; this result is discussed later. For larger airflow rates ($>$10 nl/min) the results do not show large scatter in the head loss values. After a flow rate change, the flow patterns develop relatively fast to a stationary situation. At the downstream end of the air

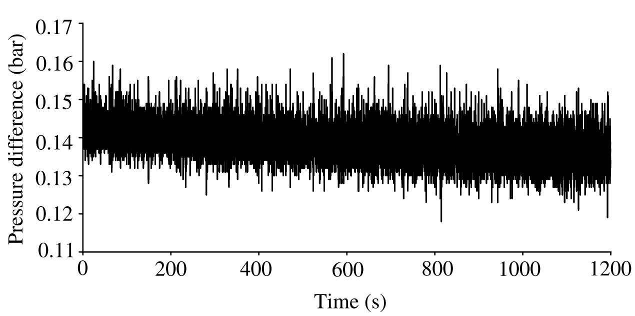

Figure 6 Air pocket growth over a period of 20 minutes

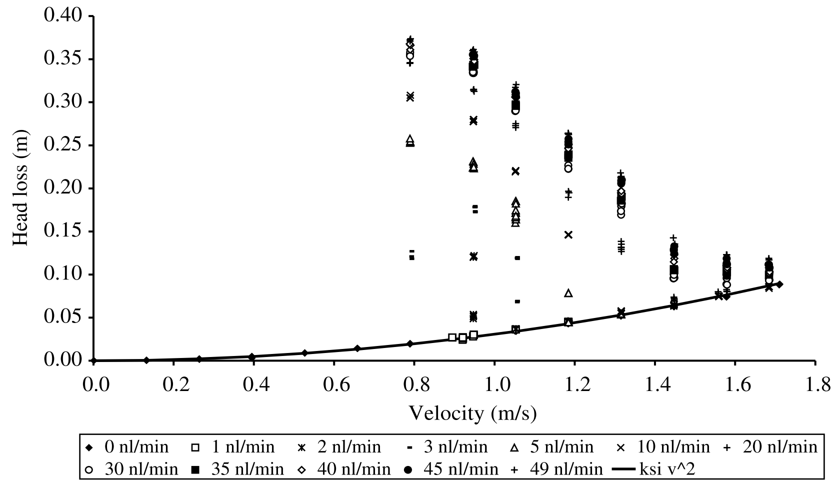

Figure 7 Total head loss as a function of the water flow rate for the 10° bend

pocket, small air bubbles move downstream while air plugs (being formed from aggregation of smaller bubbles) move upstream.

For smaller airflow rates (1 to 5 nl/min), the flow patterns may develop very slowly to a stationary situation. Transition times may go up to an hour. It is observed that the flow patterns differ at equal flow rate conditions, depending on the initial state. If small airflow rates are injected in a fully filled pipe a stationary bubble flow condition is yielded without an air pocket (Figure 5 left), resulting in little head loss. If, on the other hand, an air pocket is already formed and the airflow rate is decreased to the same small airflow rate a stationary condition is obtained with an air pocket and thus a larger head loss (Figure 5 right).

The contribution of the presence of air to the total energy loss is assessed by subtracting the energy loss of the pure water flow (the solid line in Figure 7). The contribution of the air to the energy loss is:

$$\Delta H_{total} = \frac{(p_1 - p_2)}{\rho g} - (h_1 - h_2) - \xi_{geom} \frac{v^2}{2g},$$

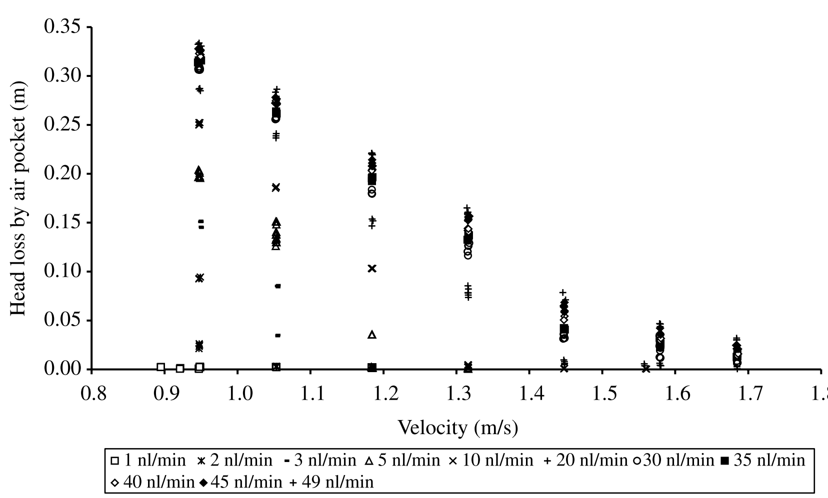

Figure 8 Head loss caused by air for the 10° bend

in which ξ_{geom} the resistance factor is for the geometry. Figure 8 shows the head loss contribution of the presence of air. The head loss at constant airflow seems to drop linearly with increasing flow rate.

The approach to the test section consists of a vertical hose followed by a 90° (in the vertical plane) steel bend. At low water flow rates, the water velocity is too small to push the air pocket through the bend. In this situation the air pocket grows in the upstream direction until the air pocket reaches the steel bend in the approach section (see Figure 2). Since a stationary condition is not reached, no measurements are taken. It is observed that for all three slopes the critical flow rate is about 35 l/s (0.95 m/s).

This can be explained by the fact that the flow has to become critical at the bend (Froude number = 1). Since the Froude number increases along the downward sloping section, the flow reaches supercritical flow and therefore 'disconnects' communication with the upstream part. In other words, the flow pattern upstream is independent from the angle of the slope downstream.

Another explanation is that the air pocket needs to grow to a certain size (in depth) before critical flow condition is reached. For lower flow rates this means that the air pocket needs to grow in upstream direction but, since it is bounded by the experimental set-up, is not able to do so. This would mean that in the case of a larger upstream section, the air could be discharged even at a lower water flow rate. Figure 1 shows the minimum velocities found so far for three different slopes that allowed air transport through the bend (solid points). In light of the discussion above, even lower critical velocities may be found.

Apart from electronic observations, also visual observation has been conducted. Using markings on the test section, the length and location of the air/water surface have been recorded. By determining the location of the phase transition, Froude number and specific energy can be assessed. These markings have been added at locations i −36, −3, 15, 42, 72, 102, 132, 162 and 212 cm. The minus sign indicates a location upstream of the bend.

Froude number and specific energy at location i are defined as follows:

$$Fr = \frac{v_i}{\sqrt{gD_h}\cos\theta} \quad \text{and} \quad E_i = y_i + \frac{Q_w^2}{2gA_i^2},$$

where v_i is the velocity, D_h the hydraulic diameter, y_i the water depth, Q_w the water flow rate and A_i the wet area. Figure 9 shows the specific energy curve for a water flow rate of 40 l/s for the 10° bend, the values measured along the air pocket from location '−34' (most left point) to '212' (most right point) and their corresponding Froude values. Similarly to free surface weirs, the free surface flow across the bend tends to go to its minimum energy level, corresponding to Froude = 1.

Discussion

This paper presents the first results of the study on air pockets in pipelines. Small air bubbles are responsible for the transport of air, while large air plugs flowing against the stream cancel out part of the air discharge at the same time. Regarding velocities that transport air, it showed that lower velocities were found than in the previous studies mentioned (see Figure 1). Further steps will be taken to improve the approaching part to the test section. This must allow measurement at water flow rates smaller than 35 l/s to assess the lowest critical velocities that discharge air.

A sufficiently high water velocity can obtain the removal of gas/air in a system. Another option is to apply air valves at the right location. At the 30° and 20° we saw that the air pocket was always located at the bend. The flow could not drive it through

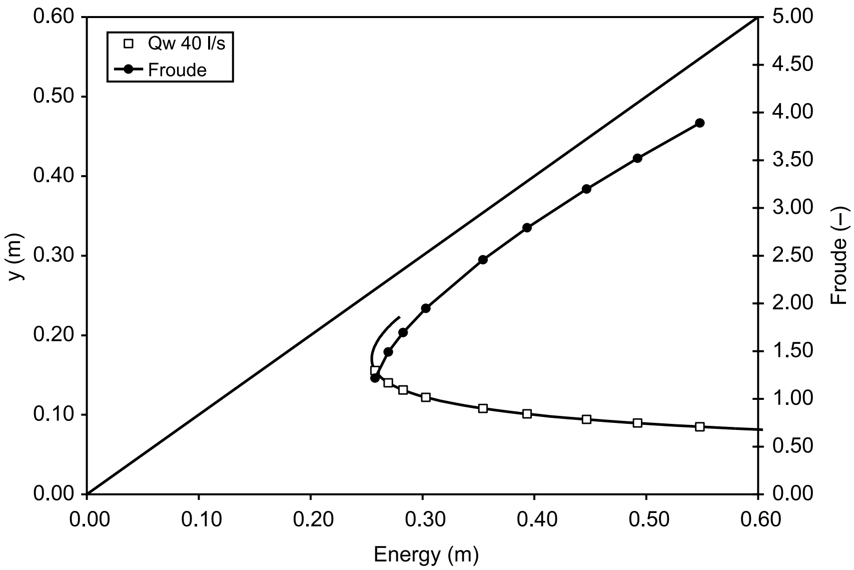

Figure 9 Specific energy curve and Froude for the 10° bend and 40 l/s

the bend. For the 10° case, the air could be driven through the bend in the case the air supply was stopped. We expect that at even smaller slopes this effect is stronger and the air pocket could be located in the sloped part. An air valve at the highest point would be ineffective for small sloped pipelines. A better understanding of the air pocket behaviour is important when designing the location of the air valves.

Further research will focus on to what extent the open channel flow properties and theory relate to the air pockets in closed conduits.

The mixing zone downstream of the air pocket shows both open channel phenomena such as the flow in a water jump but also closed conduit phenomena such as the plugs moving upstream. Further research will focus on describing these mechanisms that play a role in air transport.

Acknowledgements

The research is funded by: Foundations RIONED and STOWA, the Waterboards of Aquafin, Brabantse Delta, Delfland, DWR, Fryslân, Municipality of The Hague, Hollandse Eilanden en Waarden, Hollands Noorderkwartier, Reest en Wieden, Rivierenland, Veluwe, Zuiderzeeland and the Engineering/consultancy companies DHV and Grontmij.

References

Kent, J.C. The entrainment of air by water flowing in circular conduits with downgrade slopes, Thesis, University of California at Berkeley, California.

Walski, T.M. (1994). Hydraulics of corrosive gas pockets in force mains. *Water Environment Research*, **66**.

Wisner, P.E. (1975). Removal of air from water lines by hydraulic means. *Proceedings of the American Society of Civil Engineers, Journal of the Hydraulics Division*, **83**(HY2), February 1975.